Tumor location relative to the spleen is a prognostic factor in lymphoma patients: a demonstration from the REMARC trial

Kibrom B Girum, Anne-Ségolène Cottereau, Laetitia Vercellino, Louis Rebaud, Jérôme Clerc, Olivier Casasnovas, Franck Morschhauser, Catherine Thieblemont, Irène Buvat

Tumor location relative to the spleen is a prognostic factor in lymphoma patients: a demonstration from the REMARC trial

Kibrom B. Girum[1], Anne-Ségolène Cottereau[2], Laetitia Vercellino[3], Louis Rebaud[1,4], Jérôme Clerc[2], Olivier Casasnovas[5], Franck Morschhauser[6], Catherine Thieblemont[7], Irène Buvat[1]

[1]LITO laboratory, U1288 Inserm, Institut Curie, University Paris-Saclay, Orsay, France

[2]Department of Nuclear Medicine, Cochin Hospital, AP-HP, Paris Descartes University, Paris, France

[3]Department of Nuclear Medicine, Saint-Louis Hospital, AP-HP, Paris, France

[4]Research and Clinical Collaborations, Siemens Medical Solutions USA, 810 Innovation Dr, Knoxville, TN 37932, United states

[5]Department of Hematology, University Hospital of Dijon, Dijon, France

[6]Department of Hematology, Claude Huriez hospital, University Lille, EA 7365, Research Group on Injectable Forms and Associated Technologies, Lille, France

[7]Department of Hematology, Saint Louis Hospital, AP-HP, Paris, France

Corresponding author:

Dr. Irène Buvat

LITO laboratory, U1288 Inserm, Institut Curie, University Paris Saclay, Orsay, France

Rue Henri Becquerel, CS 90030, 91401 ORSAY Cedex, France

Mail: irene.buvat@u-psud.fr

Tel: +3362392164

ORCID iD: 0000-0002-7053-6471

First author:

Kibrom B. Girum (Ph.D.)

Postdoctoral researcher

LITO laboratory, UMR 1288 Inserm, Institut Curie, University Paris Saclay, Orsay, France

Mail: kibrom.girum@curie.fr

ORCID iD: 0000-0003-2511-0225

Funding: The REMARC clinical studies and analyses were sponsored by the Lymphoma Academic Research Organization (LYSARC) of France. This study has received funding from ANR (ANR-19-SYME-0005-03).

Word count: 4408

Running title: Tumor location is prognostic in DLBCL

ABSTRACT

Background: Baseline [^{18}F]FDG PET/CT radiomic features can improve survival prediction in patients with diffuse large B-cell lymphoma (DLBCL).

Purpose: To investigate whether characterizing tumor locations relative to the spleen location in baseline [^{18}F]FDG PET/CT images predicts survival in patients with DLBCL and improves the predictive value of total metabolic tumor volume (TMTV) and age-adjusted international prognostic index (IPI).

Methods: This retrospective study included 301 DLBCL patients from the REMARC (NCT01122472) cohort. Physicians delineated the tumor regions, while the spleen was automatically segmented using an open-access artificial intelligence algorithm (AI). We systematically measured the distance between the centroid of the spleen and all other lesions, defining the standard deviation (SD) of these distances as the lesion spread (SpreadSpleen). We calculated the maximum distance between the spleen and another lesion (Dspleen) for each patient and normalized it with the body-surface area, resulting in standardized Dspleen (sDspleen). The predictive value of each PET/CT feature for progression-free survival (PFS) and overall survival (OS) was evaluated through univariate and multivariate time-dependent Cox models and Kaplan-Meier analysis.

Results: 282 patients (mean age, 68.33 years ± 5.41 [standard deviation]; 164 men) were evaluated. The AI algorithm successfully segmented the spleen in 96% of the patients. SpreadSpleen, Dspleen, and sDspleen were neither correlated with TMTV (Pearson r <0.23) nor with IPI (r < 0.15). Using median values as cut-off, SpreadSpleen, Dspleen, and sDspleen all significantly classified patients into two-risk groups for PFS and OS (p<0.001). They complemented TMTV and IPI to classify the patients into three-risk groups for PFS and OS (p<0.001). Integrating SpreadSpleen, Dspleen or sDspleen into a Cox model based on TMTV, IPI, and TMTV combined with IPI significantly improved the concordance index for PFS and OS (p < 0.05).

Conclusion: Baseline PET/CT features that characterize tumor spread and dissemination relative to the spleen strongly predicted survival in patients with DLBCL. Integrating these features with TMTV and IPI further improved survival prediction.

Keywords: Tumor location; FDG; CT; DLBCL; Artificial intelligence

INTRODUCTION

Whole-body [^{18}F]FDG PET/CT is a standard of care for staging and assessing responses of patients with DLBCL. The CT images are often preferred to view the anatomical structures, and the [^{18}F]FDG PET images are employed to capture the molecular activities of the tumor. Despite the widespread use of the age-adjusted international prognostic index (IPI) as a prognostic index in DLBCL, recent literature suggests that image-based biomarkers could also be used for this purpose (*1*). Baseline [^{18}F]FDG PET-based features have been shown to predict survival in DLBCL patients, such as the total metabolically active tumor volume (TMTV) to characterize the tumor burden (*1–4*). Recently introduced tumor dissemination features, the distance between the two farthest lesions (Dmax) and the maximum distance between the largest lesion and another lesion (Dbulk), have shown promising results to predict survival (*5–9*). Their simplicity, intuitive interpretation, and predictive value of the outcome inspired this study.

Given that the spleen plays a particular role in the lymphatic system and particularly in DLBCL (*10*), we assumed that the spleen could serve as a reference organ to model the disease distribution and dissemination over the whole-body.

The purpose of this study was to investigate whether tumor distribution and dissemination measured relative to the spleen from baseline [^{18}F]FDG PET/CT images had prognostic values independent of that of TMTV and IPI and improved survival prediction in DLBCL patients. The individual prognostic values of these new image-based features were evaluated in terms of progression-free survival (PFS) and overall survival (OS). We also assessed the added prognostic value of these biomarkers when they are combined with TMTV and age-adjusted IPI.

MATERIALS AND METHODS

Patients

A retrospective analysis of 301 DLBCL patients with a baseline [^{18}F]FDG PET/CT scan from the REMARC trial (NCT01122472) was conducted. The REMARC trial study started including patients in 2010 and was a double-blind, international, multicenter, randomized phase II study. Patients included in this study were 60-80 years old, had Ann Arbor stage I-IV and age-adjusted IPI ≥ 1 at diagnosis, with histologically proven CD20+ DLBCL according to 2008 world health organization criteria (*11*) . Detailed characteristics of the patient were reported elsewhere (*2*). The survival outcomes (PFS and OS) were recorded as defined by the revised National Cancer Institute criteria (*12*). Figure 1 summarizes the flow diagram of the data. Patient data were anonymized before any analysis. All patients had given written informed consent, and institutional review board approval, including ancillary studies, was obtained. The demographics and staging of the DLBCL patients used for the survival analysis are summarized in Table 1.

Image Analysis and Features Extraction

Experienced nuclear medicine physicians (AS.C - 7 year experience and L.V - 10 year experience) delineated the lesion regions semi-automatically from the baseline 3-dimensional PET/CT images. The exact delineation procedure has been previously described (*2*). All lesion segmentations were visually verified to include pathological lesions and exclude physiological uptakes. The total volume of the lesions for each patient was then calculated as TMTV. Two recently introduced lesion dissemination features, Dmax (distance between two farthest lesions) (*6*) and Dbulk (maximum distance between the largest lesion and another lesion) (*7*) were calculated from each lesion's centroid.

Automatic spleen segmentation on CT images: An artificial intelligence (AI) method called TotalSegmentator was used to segment the spleen from 3-dimensional CT images (*13*). This method was initially developed to segment 104 anatomical structures from CT images but in our work, we focused on spleen segmentation only. A post-processing method was developed to check the quality of the spleen segmentation and correct it when needed. The post-processing method included two criteria to trigger a warning: ensuring that the spleen segmentation had a single connected component and was not outside the whole-body field of view. If the spleen included more than one connected component, the largest one was automatically selected as the spleen. After post-processing, all segmentations were visually verified and manually adjusted using the LIFEx software whenever needed (*14*). As the CT and PET images were aligned from the PET/CT acquisition, for each patient, the spleen segmentation result obtained from the AI was superimposed onto the lesion segmentation obtained from the experts. Figure 2 illustrates the proposed image processing pipeline.

PET/CT features extraction: The superimposed spleen and lesion 3-dimensional regions were used to calculate the tumor location relative to the spleen. From the 3-dimensional coordinates of the spleen region, the centroid was automatically calculated and defined the spleen location. For each patient, the distance between the centroid of the spleen $A = (x_a, y_a, z_a)$ and all other detected lesions' centroids ($B_i = x_{bi}, y_{bi}, z_{bi}$, centroid of the i^{ith} lesion) was measured using the Euclidean distance formula $\sqrt{(x_{bi} - x_a)^2 + (y_{bi} - y_a)^2 + (z_{bi} - z_a)^2}$, $i = 1, 2, 3 \ldots, N$, for N detected lesions. The standard deviation of the distance between the spleen centroid and all lesions was calculated for each patient as $\sigma = \sqrt{\frac{\sum_{i=1}^{N}(ABi - \mu)^2}{N}}$ and referred to as lesion spread relative to the spleen (SpreadSpleen), where $\mu = \sum_{i=1}^{N}(AB_i)/N$. The distance between the spleen and the farthest lesion from the spleen (Dspleen) was deduced for each patient and normalized by the patient body surface area (BSA), given by $BSA =$

$\frac{\sqrt{weight\ (kg) * height\ (cm)}}{60}$, and named hereafter the standardized distance of the farthest lesion from the spleen (sDspleen) (*15*). Supplemental Figure 1 illustrates the definitions of the new features relative to the spleen. The image processing pipeline, including the AI-based spleen segmentation, features extraction, and survival analysis, will be made publicly available upon publication [Anonymized website].

The exact same analysis was performed using the liver as a reference organ, as described in the Supplemental data.

Statistical Analysis

The predictive power of the calculated features was evaluated in univariate and multivariate analyses. First, we evaluated if each of the calculated biomarkers was predictive of the PFS and OS using Kaplan-Meir survival analysis and a time-dependent area under the receiver operating characteristics curve (AUC) and the results obtained for the different features were compared. Correlations between the biomarkers were calculated using the Pearson correlation coefficient (rho). Second, we evaluated the added values of the predictive biomarkers combined with known predictive biomarkers, including the TMTV and the IPI. A multivariate Cox regression analysis with a bootstrap resampling at the patient level was employed to associate confidence intervals (CIs) to the Cox model hazard ratio (HR) and the concordance index (C-index). The empirical 95% confidence interval (CI) was reported with a bootstrap of 5000 random samplings with replacement. Cox proportional hazard models were used to analyze univariate and multivariate results. P-values less than 0.05 were interpreted as statistically significant.

RESULTS

Among the 301 patients from the REMARC cohort, 282 patients (mean age ± SD, 68.33 ± 5.41, y; 164 men) were included for the biomarker and survival analysis. [^{18}F]FDG PET/CT quality control and other

criteria described in Figure 1 excluded 19 patients. The characteristics of the 282 patients included for the survival analysis are shown in Table 1.

Spleen segmentation: Among the 295 patients available for PET/CT segmentations (regardless of the availability of survival data, Figure 1), the TotalSegmentator AI method correctly detected and segmented the spleen in 282 patients (96%), the post-processing method yielded warning in 13 patients (4%) and automatically corrected the segmentation in 12 of those 13 patients. The spleen segmentation of one patient only had to be manually corrected using the LIFEx software. The median size of the spleen was 256.15 mL (interquartile range (IQR): 169 - 395). 101 (34%) patients had lesions segmented by the expert in the spleen. Figure 3 shows the coronal maximum intensity projection (MIP) views of the PET image of one patient, the PET image overlapped with the spleen segmentation by the AI model, and the lesion segmentations by the expert. The automatically calculated centroid of the spleen is shown as a crosshair.

PET/CT features: Table 2 shows the descriptive statistics of the baseline PET/CT features in the 282 patients. Neither the standardized maximum distance between the spleen and another lesion (sDspleen) nor the lesion spread (SpreadSpleen) were correlated with TMTV (Spearman rho=0.14 and 0.21 respectively) or IPI (rho=0.12 and 0.15). The correlation between sDspleen and SpreadSpleen was 0.68. All dissemination features were moderately correlated pairwise (rho=0.60-0.78). The correlogram between all PET/CT features is given in supplemental Figure 2.

Univariate survival analysis: The median values of Dspleen, sDspleen, and SpreadSpleen shown in Table 2 were used as cut-off values for the Kaplan-Meier survival analysis. Each feature reflecting the tumor location relative to the spleen (Dspleen, sDspleen and SpreadSpleen) classified the patients into

two-risk groups (high-risk and low-risk) significantly for both PFS and OS (log-rank test $p<0.001$), see supplemental Figure 3. Using the optimal cutoff values obtained by maximizing the Youden index of a receiver-operating characteristic curve, all biomarkers were predictive of PFS and OS (log-rank test $p<0.05$). Of the 73 (26%) patients with PFS less than 4-years, 51 (70%) patients had also Dspleen greater than the median value (32.43 cm), and 52 (71%) patients had TMTV greater than the median value (242 cm^3). The Harrell's concordance index (C-index) for PFS (OS) were 0.66 (0.66) for TMTV, 0.64 (0.60) for Dmax, 0.62 (0.60) for Dbulk, 0.65 (0.63) for SpreadSpleen, 0.66 (0.64) for Dspleen, 0.65 (0.64) for sDspleen, 0.63 (0.63) for tumor spread measured from the liver (SpreadLiver), 0.63 (0.63) for the distance between the liver and the farthest lesion from the liver (Dliver), and 0.63 (0.63) for the standardized Dliver (sDliver), and 0.59 (0.61) for IPI.

The time-dependent receiver-operating characteristics curve (AUC) and hazard ratios (HR) with 95% confidence interval (CI) of the image-based biomarkers are shown in Table 3. The sDspleen method scored the highest for predicting both OS and PFS in terms of hazard ratios. All PET features and the IPI were predictive of survival in patients with DLBCL, as indicated by their AUC (AUC ≥ 0.60), and their predictive values were all statistically significant ($p < 0.05$).

Multivariate survival analysis: Three risk categories can be significantly distinguished by combining the TMTV with the Dspleen or sDspleen (Figure 4). See supplemental Figure 4 for the SpreadSpleen, Dmax, and Dbulk features. For simplicity, we used the median values as cut-off values in the Kaplan-Meier analysis for these three features, while the optimal TMTV value of 220 cm^3 previously published was used (*9*). The sDspleen values were scaled by 100 for computational purposes.

Results from multivariate Cox regression analyses are shown in Table 4. We consider three baseline models to evaluate the added predictive value of the new PET/CT features with respect to the known biomarkers. The baseline models were based on TMTV, IPI, and TMTV combined with IPI. The added survival predictive values were evaluated using the concordance index (C-index). Only Dbulk had no significant change in the C-index ($p>0.05$) when combined with the TMTV for OS prediction. In all scenarios, regardless of the baseline model, the tumor location relative to the spleen (Dspleen, sDspeen and SpreadSpleen) features significantly improved the predictive power of the IPI, TMTV, and TMTV combined with IPI ($p<0.05$). The highest concordance indexes were achieved when the spleen location-based features (SpreadSpleen, Dspleen and sDspleen) were combined with TMTV and the combined model of the TMTV and IPI.

Supplemental Figure 3 (D) demonstrates that lymphoma splenic invasion is also a poor prognosis factor, with log-rank test $P = 0.03$ for PFS and OS. In the subgroup of patients without splenic invasion (n=185), the proposed spleen-based biomarkers were prognosticators (supplemental Figure 5). The results in supplemental Table 1 further confirm the improved added predictive values of the spleen-based features to the combined model of TMTV with IPI in patients without splenic invasion.

DISCUSSION

We developed and evaluated a new framework to extract novel PET/CT features that characterize how tumors spread and disseminate relative to the spleen in patients diagnosed with DLBCL and demonstrated the additional prognostic values of these features compared to known prognostic features. Lymphoma is a cluster of blood cancers that develop from lymphocytes and can spread to various body parts through the circulatory system. The spleen, an essential organ in blood filtration, plays a crucial role for removing old or damaged red blood cells, pathogens, and other foreign particles. The spleen also acts

as a reservoir for the immune cells and platelets, which are critical for fighting infections and blood clotting.

The specific role of the spleen in the lymphatic system (*10*) was the primary motivation for considering the spleen as a reference organ to model disease spread and dissemination. We therefore investigated the possibility of simple and interpretable features that could characterize the location of the lesions relative to the spleen in patients with DLBCL. Lesion location-based features are often less sensitive to variations in imaging modalities or imaging devices and segmentation methods once the lesions are identified, which is an asset to transfer from academic research to routine clinical practice (*8*).

This study introduces three new features (SpreadSpleen, Dspleen and sDspleen) extracted from baseline PET/CT images to quantify tumor locations relative to the spleen. Previous studies have proven that PET/CT-based features can be used for patient management on different DLBCL cohorts (*9*). No previous studies have been conducted to model the disease distribution and dissemination relative to a reference organ. Here, we used an open-access fully automated AI algorithm to segment the spleen from the CT images (*13*). The segmentation results were carefully assessed and in 96% (282 of 295) of the patients, the spleen segmentation was acceptable. A correction was needed for only 4% (13 of 295) of the patients. Our new features are based on the centroid of the spleen, which makes them barely sensitive to the precise delineation of the spleen. We checked this lack of sensitivity to the exact delineation of the spleen by randomly shifting the spleen centroid by 2 cm and observed no substantial changes in prognostic values of the spleen-based biomarkers (results provided in the supplemental material). Experts performed lesion segmentations in our study. However, to fully automate the process, the pipeline could be integrated with existing AI-based automatic lesion segmentations from PET/CT images (*16*–*19*).

Univariate and multivariate Kaplan-Meier and Cox-model analyses showed that SpreadSpleen, Dspleen and sDspleen are strong predictors of PFS and OS. They can significantly classify patients with DLBCL into two-risk groups (high and low-risk) using the median values as cut-off values. Experimental results showed that Dspleen predicts PFS and OS like sDspleen. In cases of missed BSA in clinical information, Dspleen could be used. SpreadSpleen, Dspleen and sDspleen features can be calculated for any patient, including those with a single lesion. They consistently and significantly improved the predictive power of the IPI, TMTV, and IPI combined with TMTV. The improvements were more significant than those brought by other lesion dissemination-based features (Dmax and Dbulk). It demonstrates that the spleen-based features can complement TMTV and IPI to better characterize the disease at an early stage.

The proposed spleen-based features (SpreadSpleen, Dspleen and sDspleen) are simple to calculate and intuitive to interpret. The spleen was chosen as the reference organ due to its role in the lymphatic system. Lymphoma splenic invasion is also a poor prognosis factor. In subgroups of patients without splenic invasion, the spleen-based features were prognosticators, suggesting that the spleen-based features code more than just a patient's splenic invasion or not. The bladder and liver were also tested as reference organs for evaluating tumor distribution and dissemination features. The predictive value from the bladder-based features was low for both PFS and OS (AUC < 0.60, data not shown). Although liver-based features were correlated with spleen-based features due to their relative anatomical proximity and were also predictive (data in the supplemental material), spleen-based features always had significantly higher predictive values ($p<0.05$).

The main limitation of our study is the need for further evaluation of the proposed new features, ideally in multicenter cohorts, to confirm our findings. In addition, developing a machine learning model

that would best combine all PET/CT prognostic features to improve the prediction of PFS and OS warrants further investigation.

CONCLUSION

In this study, we introduced three predictive biomarkers extracted from baseline PET/CT images in patients with DLBCL. To our knowledge, this is the first study showing that characterizing tumor location relative to a reference organ predicts survival in a large series of DLBCL. We demonstrated that characterizing how the tumor spreads and disseminates relative to the spleen can improve survival prediction (PFS and OS) compared to the internationally accepted risk score method, age-adjusted IPI, and PET/CT image-based biomarker, TMTV, for patients with DLBCL.

DISCLOSURE

Kibrom B. Girum and Irène Buvat disclosed a research grant given to the Institut Curie by ANR (ANR-19-SYME-0005-03). Louis Rebaud disclosed employment by Siemens Medical Solutions. No other potential conflicts of interest relevant to this article exist.

KEY POINTS

QUESTION: Do baseline [^{18}F]FDG PET/CT features that characterize the tumor location relative to a reference organ predict survival in patients with DLBCL and can they improve the predictive value of the total metabolic tumor volume (TMTV) and age-adjusted international prognostic index (IPI)?

PERTINENT FINDINGS: New baseline PET/CT features characterizing tumor spread (SpreadSpleen) and dissemination (Dspleen) relative to the spleen predicted progression-free and overall survival (PFS and

OS) in DLBCL patients. The new biomarkers significantly enhanced the predictive value of TMTV and IPI for both PFS and OS.

IMPLICATIONS FOR PATIENT CARE: Tumor spread (SpreadSpleen) and dissemination (Dspleen) features relative to the spleen calculated from baseline [^{18}F]FDG PET/CT are prognostic biomarkers in patients with DLBCL.

REFERENCES

1. Mikhaeel NG, Heymans MW, Eertink JJ, et al. Proposed New Dynamic Prognostic Index for Diffuse Large B-Cell Lymphoma: International Metabolic Prognostic Index. *J Clin Oncol*. 2022;40:2352-2360.
2. Vercellino L, Cottereau A, Casasnovas O, et al. High total metabolic tumor volume at baseline predicts survival independent of response to therapy. *Blood*. 2020;135:1396-1405.
3. Thieblemont C, Chartier L, Dührsen U, et al. A tumor volume and performance status model to predict outcome before treatment in diffuse large B-cell lymphoma. *Blood Adv*. 2022;6:5995-6004.
4. Eertink JJ, Zwezerijnen GJ, Heymans M, et al. Baseline PET radiomics outperform the IPI risk score for prediction of outcome in diffuse large B-cell lymphoma. *Blood*. 2023;141:3055-3064.
5. Ceriani L, Zucca E. D max : A simple and reliable PET/CT-derived new biomarker of lymphoma outcome? *Hematol Oncol*. 2022;40:843-845.
6. Cottereau A-S, Nioche C, Dirand A, et al. 18 F-FDG PET Dissemination Features in Diffuse Large B-Cell Lymphoma Are Predictive of Outcome. *J Nucl Med*. 2020;61:40-45.
7. Eertink JJ, van de Brug T, Wiegers SE, et al. 18F-FDG PET baseline radiomics features improve the prediction of treatment outcome in diffuse large B-cell lymphoma. *Eur J Nucl Med Mol Imaging*. 2022;49:932-942.
8. Albano D, Treglia G, Dondi F, et al. 18F-FDG PET/CT Maximum Tumor Dissemination (Dmax) in Lymphoma: A New Prognostic Factor? *Cancers (Basel)*. 2023;15:2494.
9. Cottereau A-S, Meignan M, Nioche C, et al. Risk stratification in diffuse large B-cell lymphoma using lesion dissemination and metabolic tumor burden calculated from baseline PET/CT†. *Ann Oncol*. 2021;32:404-411.
10. Mebius RE, Kraal G. Structure and function of the spleen. *Nat Rev Immunol*. 2005;5:606-16.

11. Thieblemont C, Tilly H, Gomes da Silva M, et al. Lenalidomide Maintenance Compared With Placebo in Responding Elderly Patients With Diffuse Large B-Cell Lymphoma Treated With First-Line Rituximab Plus Cyclophosphamide, Doxorubicin, Vincristine, and Prednisone. *J Clin Oncol*. 2017;35:2473-2481.

12. Cheson BD, Pfistner B, Juweid ME, et al. Revised Response Criteria for Malignant Lymphoma. *J Clin Oncol*. 2007;25:579-586.

13. Wasserthal J, Breit H-C, Meyer MT, et al. TotalSegmentator: Robust Segmentation of 104 Anatomic Structures in CT Images. *Radiol Artif Intell*. July 2023.

14. Nioche C, Orlhac F, Boughdad S, et al. Lifex: A freeware for radiomic feature calculation in multimodality imaging to accelerate advances in the characterization of tumor heterogeneity. *Cancer Res*. 2018;78:4786-4789.

15. R D Mosteller. Simplified Calculation of Body-Surface Area. *N Engl J Med*. 1987;317:1098-1098.

16. Blanc-Durand P, Jégou S, Kanoun S, et al. Fully automatic segmentation of diffuse large B cell lymphoma lesions on 3D FDG-PET/CT for total metabolic tumour volume prediction using a convolutional neural network. *Eur J Nucl Med Mol Imaging*. 2021;48:1362-1370.

17. Sibille L, Seifert R, Avramovic N, et al. 18 F-FDG PET/CT Uptake Classification in Lymphoma and Lung Cancer by Using Deep Convolutional Neural Networks. *Radiology*. 2020;294:445-452.

18. Girum KB, Rebaud L, Cottereau A-S, et al. 18 F-FDG PET Maximum-Intensity Projections and Artificial Intelligence: A Win-Win Combination to Easily Measure Prognostic Biomarkers in DLBCL Patients. *J Nucl Med*. 2022;63:1925-1932.

19. Jemaa S, Fredrickson J, Carano RAD, Nielsen T, de Crespigny A, Bengtsson T. Tumor Segmentation and Feature Extraction from Whole-Body FDG-PET/CT Using Cascaded 2D and 3D Convolutional Neural Networks. *J Digit Imaging*. 2020;33:888-894.

FIGURES AND TABLES

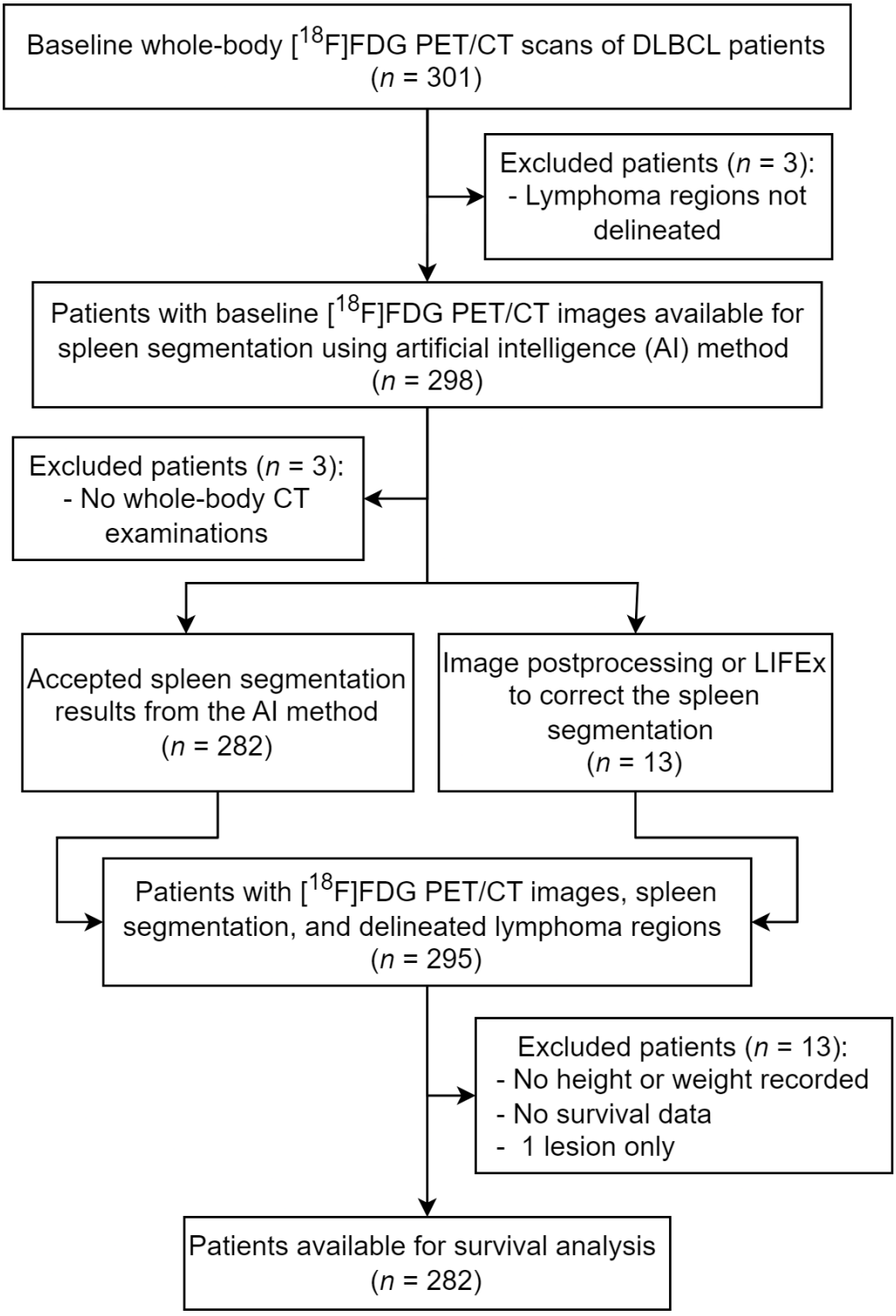

FIGURE 1. Study flowchart. FDG = fluorodeoxyglucose.

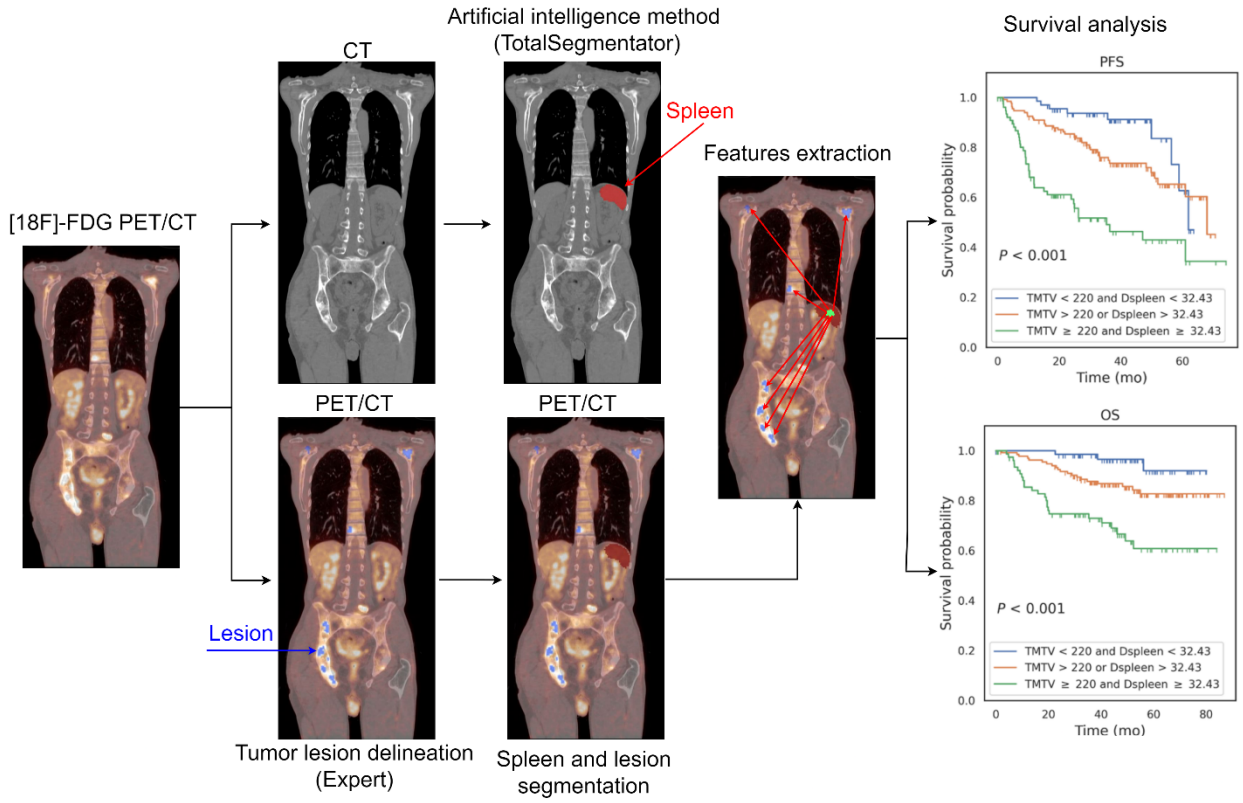

FIGURE 2. Overview of the image processing pipeline to calculate the tumor locations relative to the spleen from [^{18}F]FDG PET/CT images. The deep learning-based whole-body segmentation (Totalsegmentator) was used to segment the spleen from the CT images. From the overlapped tumor and spleen segmentations, we extracted whole-body radiomic features, including total metabolic tumor volume (TMTV) and distance between the spleen and farthest lesion (Dspleen). The extracted radiomic features were used to predict overall survival (OS) and progression-free survival (PFS).

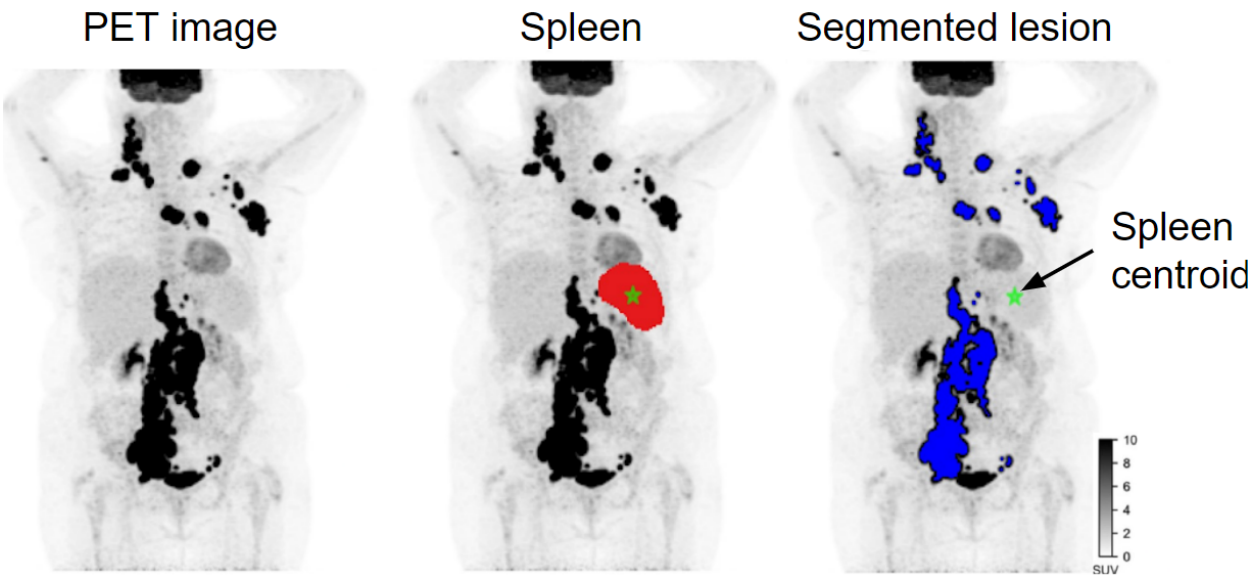

FIGURE 3. Maximum intensity projection (MIP) of the PET images with the spleen segmentation by the AI model and lesion segmentations by the expert. The crosshair indicates the centroid of the spleen.

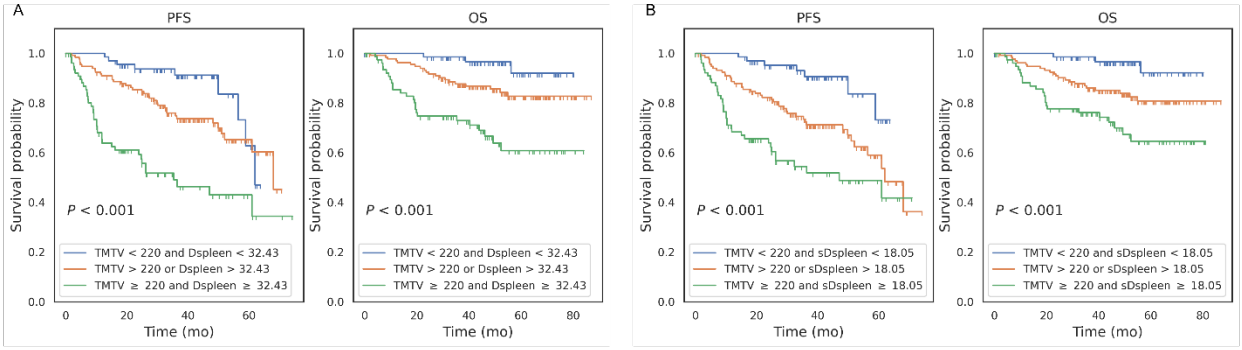

FIGURE 4. Three-risk category Kaplan-Meier curves of the OS and PFS according to the total metabolic tumor volume (TMTV (cm^3) with the distance between the spleen and the lesion farthest from the spleen (Dspleen cm) (A), and standardized Dspleen (sDspleen*100 m^{-1}) (B).

TABLES

TABLE 1. Population characteristics (n = 282)

Sex	
No. of men	164 (58.2%)
No. of women	118 (41.8%)
Median age (y)	68 .33 [64.0-73.0]
Median weight (kg)	72 [63.0-83.0]
Median height (cm)	168 [160.0-175.0]
Ann Arbor stage	
<I	1 (0.4%)
>=II	281 (99.6%)
Performance status	
0	114 (40.4%)
1	120 (42.6%)
2	41 (14.5%)
3	2 (0.7%)
4	2 (0.7%)
Missing	3 (1.1%)
Note: data in brackets are interquartile ranges (quartile one to quartile three).	

TABLE 2. Statistics of the PET/CT features.

PET/CT features	Mean	Standard deviation (SD)	Median	Range (Q1-Q3)
TMTV (cm^3)	434.43	569.52	240.02	78.24 -551.08
SpreadSpleen (cm)	6.30	3.03	6.67	3.99-8.41
Dspleen(cm)	32.02	9.57	32.43	25.92-38.73
sDspleen *100 (m^{-1})	17.59	5.45	18.05	13.80-21.29
Dmax (cm)	44.08	23.05	44.62	23.84-64.17
Dbulk (cm)	31.63	18.62	31.73	15.63-44.40

TABLE 3. Univariate analysis of the predictive value of PET/CT features in time-dependent receiver-operating characteristics curve (AUC) and hazard ratios (HR), mean (95% confidence interval). Progression-free survival (PFS), overall survival (OS).

Clinical and PET/CT features		PFS		OS	
		AUC	HR	AUC	HR
Known features	IPI	0.60 (0.5-0.7)	3.45 (1.1-8.7)	0.61 (0.5-0.7)	6.18 (1.5-17.4)
	TMTV	0.67 (0.6-0.7)	12.03 (2.2-57.6)	0.67 (0.6-0.8)	18.16 (2.6-108.2)
	Dmax	0.64 (0.6-0.7)	7.87 (2.0-18.9)	0.62 (0.5-0.7)	7.39 (1.4-18.4)
	Dbulk	0.63 (0.6-0.7)	5.59 (1.6-14.1)	0.62 (0.5-0.7)	6.96 (1.3-18.2)
New features	SpreadSpleen	0.64 (0.6-0.7)	5.85 (1.6-15.2)	0.63 (0.5-0.7)	9.87 (1.7-31.5)
	Dspleen	0.66 (0.6-0.7)	17.49 (3.6-60.5)	0.64 (0.5-0.7)	18.18 (2.3-54.7)
	sDspleen	0.66 (0.6-0.7)	53.28 (10.0-181.0)	0.65 (0.6-0.7)	32.51 (2.2-348.5)

TABLE 4. The predictive value of PET/CT features, combined with known features (TMTV and IPI) as a baseline Cox model, mean (95% confidence interval). Concordance index (C-index).

PET/CT features	PFS (C-index)	Increase in C-index	OS (C-index)	Increase in C-index
IPI (baseline)	*0.58 (0.5-0.6)*		*0.61(0.5-0.7)*	
IPI + TMTV	0.65 (0.6-0.7)	0.07	0.67(0.6-0.7)	0.07
IPI + Dmax	0.65(0.6-0.7)	0.07	0.65(0.5-0.7)	0.04
IPI + Dbulk	0.65(0.6-0.7)	0.06	0.66(0.6-0.7)	0.05
IPI + SpreadSpleen	0.67(0.6-0.7)	0.08	0.68(0.6-0.8)	0.08
IPI + Dspleen	**0.68(0.6-0.7)**	0.09	**0.69(0.6-0.8)**	0.08
IPI + sDspleen	0.67(0.6-0.7)	0.09	0.68(0.6-0.8)	0.08
TMTV (baseline)	*0.66(0.6-0.7)*		*0.67(0.6-0.8)*	
TMTV + Dmax	0.67(0.6-0.7)	0.01	0.67(0.6-0.7)	-0.01
TMTV + Dbulk	0.67(0.6-0.7)	0.01	0.67(0.6-0.7)	0.00
TMTV + SpleenSpread	0.69(0.6-0.7)	0.03	0.70(0.6-0.8)	0.03
TMTV + Dspleen	0.69(0.6-0.7)	0.03	0.70(0.6-0.8)	0.03
TMTV + sDspleen	**0.69(0.6-0.8)**	0.03	**0.71(0.6-0.8)**	0.04
TMTV + IPI (baseline)	*0.65(0.6-0.7)*		*0.67(0.6-0.7)*	
TMTV + IPI + Dmax	0.67(0.6-0.7)	0.02	0.68(0.6-0.7)	0.00
TMTV + IPI + Dbulk	0.67(0.6-0.7)	0.02	0.68(0.6-0.8)	0.01
TMTV + IPI + SpreadSpleen	0.69(0.6-0.7)	0.04	0.71(0.6-0.8)	0.03
TMTV + IPI + Dspleen	0.69(0.6-0.7)	0.04	0.71(0.6-0.8)	0.03

TMTV + IPI + sDspleen	0.69(0.6-0.7)	0.04	0.71(0.6-0.8)	0.04

Graphical Abstract

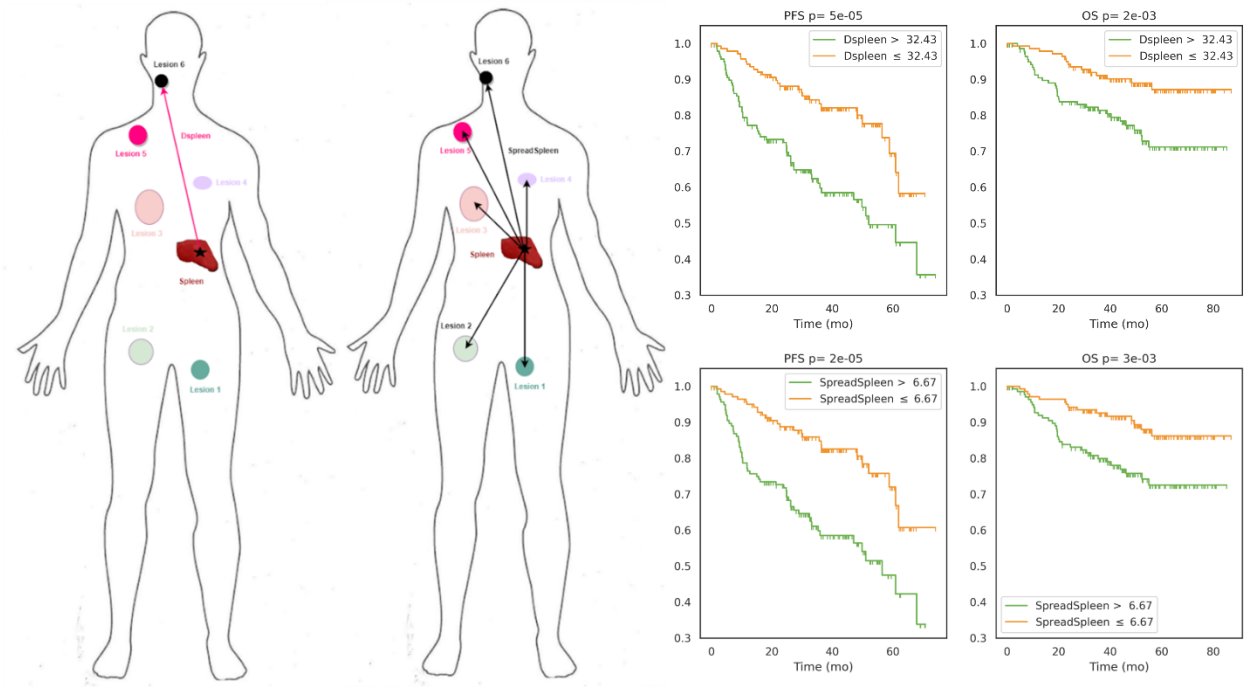

Dspleen SpreadSpleen Survival analysis (PFS and OS)